Hindawi
Advances in Civil Engineering
Volume 2021, Article ID 8858874, 18 pages
https://doi.org/10.1155/2021/8858874

Research Article

Study on the Generalized Displacement Boundary and Its Analytical Prediction for Ground Movements Induced by Shield Tunneling

Qianlong Tang,[1] Fudong Chen,[2] Mingfeng Lei,[1,2] Binbin Zhu,[1] and Limin Peng[1]

[1]*School of Civil Engineering, Central South University, Changsha 410075, China*
[2]*Key Laboratory of Engineering Structure of Heavy Haul Railway (Central South University), Changsha 410075, China*

Correspondence should be addressed to Mingfeng Lei; mingdfenglei@csu.edu.cn and Binbin Zhu; zhubinbin@csu.edu.cn

Received 25 September 2020; Revised 23 February 2021; Accepted 3 March 2021; Published 23 March 2021

Academic Editor: Gang Zhou

The process of shield tunnel excavation would inevitably cause surrounding ground movement, and excessive displacement in the soil could lead to large deformation and even collapse of the tunnel. The methods estimating convergence deformation around tunnel opening is summarized. Then, a universal pattern of displacement boundary condition around the tunnel cavity is originally introduced, which is solved as the combination of three fundamental deformation modes, namely, uniform convergence, vertical translation, and ovalization. The expression for the above-mentioned displacement boundary condition is derived, by imposing which the analytical solution for ground movements, based on the stress function method, is proposed. The reliability and applicability of this proposed solution are verified by comparing the observed data in terms of surface settlement, underground settlement, and horizontal displacement. Further parametric analyses indicate the following: (1) the maximum settlement increases linearly with the gap parameter and the tunnel radius, while it is negatively related to the tunnel depth; (2) the trough width parameter is independent of the gap parameter and the radius, while it is proportional to the tunnel depth. This study provides a new simple and reliable method for predicting ground movements induced by shield tunneling.

1. Introduction

Over the last decade, an increasing urbanization has led to the over-crowded ground transportation issue around the world [1–3]. In order to alleviate the surface traffic congestion, underground subway construction has gained rapid development, in which shield tunneling method is widely applied due to its advantages (e.g., automation, all-weather, and widespread applicability) [4–6]. However, the process of shield tunnel excavation would inevitably disturb the original stress state of surrounding soil and cause its horizontal displacement and subsidence, which could even damage neighboring surface structures [7–9]. Therefore, it is of great significance to predict ground movements induced by tunneling, especially for the cases of tunneling under intense buildings, in order to assess the potential correlated damage of surface structures [1, 10–12].

The development of prediction methods to calculate tunnel-induced ground movement is among the hottest topics in tunnel engineering [13]. A large number of research efforts have been paid with respect to methods for predicting tunneling-induced ground movements. Generally, they can be classified into three categories: empirical [14–17], numerical [18–22], and analytical [23–30]. Empirical formulas are principally obtained based on field observations and intuitive deductions, such as the Peck formula [17], which is able to accurately reflect transverse settlement profile. However, these empirical methods are usually lacking rigorous theoretical derivations and thus result in very limited applicability. On the other hand, numerical approach has been greatly used for predicting ground movements, because it can accurately simulate tunnel excavation processes under various geological conditions. However, the numerical analyses often produce unsatisfied results, due to insufficient

information of in situ conditions and unrealistic modeling of soil behavior. In addition, advanced computing equipment is required and a large amount of computation time is needed for such analysis. For the analytical method, it adopts assumptions concerning the calculation model and constitutive behavior of soil, satisfying principles of mechanics and rigorous mathematical deduction. Furthermore, extensive parametric analysis is much easier to be carried out using the analytical method.

Benefiting the aforementioned advantages, the analytical method has then become the primary approach to compute tunneling-induced ground movements. Generally, this method is conducted by developing mathematical equations satisfying soil behavior and solving them based on special boundary conditions. The analytical methods for predicting tunnel-induced ground movements cover four main categories: the virtual image technique [23–25, 31], the complex variable method [26, 32–34], the stochastic medium theory [27, 35, 36], and the stress function method [28–30, 37, 38]. Among them, the stress function method may develop solutions lacking physical meaning, for a function $\ln r$ existing, which does not meet the common condition of $U_{r(\theta)}|_{r(\theta)\longrightarrow\infty}\longrightarrow 0$, where $U_{r(\theta)}$ refers to the ground movement in the radial or hoop direction. And thus mathematical correction must be taken, such as the boundary of zero vertical displacement introduced by Chou and Bobet [38] and modifying the expressions by using $-U_\theta$ instead of U_θ recommended by Park [28], which leads to considerably smaller settlement far away from the excavation face, larger ground uplift, and narrower settlement trough than the observed results.

The boundary condition is imposed and then the closed form solution is developed. Two types of boundary conditions are classified: the far end and the near end (namely, around the tunnel opening). For the former case, the boundary condition far from the tunnel opening is physically based on the initial stress state. For the latter case, the boundary of the tunnel opening can be divided into two kinds: the stress boundary and the displacement boundary. These two boundary conditions are developed based on ground-liner interaction mechanism and convergence deformation pattern around the tunnel section, respectively [39]. Usually the radial stress at the tunnel opening is assumed to be zero, while the stress at the ground-liner interface can be determined in case of the consideration of ground-liner interaction. However, the displacement boundary is ambiguous because of the varied convergence deformation patterns under different geological conditions, and construction techniques [40].

In order to describe the deformation at tunnel cavity, Sagaseta [23] suggested a uniform radial convergence pattern (Figure 1(a)); this is, only uniform radial ground movement is considered. However, the practical deformation around the tunnel opening is highly non-uniform due to soil pressure and construction quality; and it is noted that the simplified pattern results in wider settlement trough and larger horizontal displacement than the observed deformation shape. Verruijt and Booker [40] extended the model suggested by Sagaseta [23] and proposed an oval-shaped pattern, as shown in Figure 1(b). But this mode may lead to a wider settlement trough and smaller settlements. On the other hand, Rowe and Kack [42] stated that the radial ground movement around the tunnel opening is not uniform (Figure 1(c)), because the gap (tail void) around the tunnel is non-circular. Loganathan and Poulos [25] took into account this nonuniform radial movement by introducing an equivalent ground-loss parameter, which can be estimated with respect to the gap parameter proposed by Lee et al. [43]. This deformation pattern may calculate a smaller maximum settlement in some cases because the deformation of liner is neglected.

Further researches and numerous practices pointed out that the deformation at the tunnel cavity can be considered as the sum of three above-mentioned modes [40]. Based on this, Park [28] presented four boundary conditions of the empirically prescribed displacement around the tunnel. Tong et al. [30] and Zhang et al. [29] further summarized the deformation pattern around the tunnel and separately proposed a kind of displacement boundary condition by contrast analysis with three empirically appointed displacements at the tunnel opening. To sum up, as for analytical prediction for tunneling-induced ground movement, limitations still exist for both the stress function method and displacement boundary condition, and further researches are still needed to be conducted.

Looking at these challenges, this paper originally introduces a universal pattern of displacement boundary condition around the tunnel cavity (defined as the generalized displacement boundary herein) based on the three fundamental deformation modes. An optimal plane analysis model is chosen to avoid mathematical correction for the results. Then, an analytical method to compute ground movements induced by shield tunneling is proposed based on the stress function method by imposing the generalized displacement boundary condition. The analytical method is validated against a set of 20 field cases with monitoring data. The method associated with engineering properties is finally introduced to estimate the characteristic parameters of the generalized displacement boundary.

2. The Generalized Displacement Boundary

2.1. Basic Assumptions. Generally, the time is short between shield excavation and liner installation, so is the time for compatible deformation between soil and liner. At this point, the pore water pressure is slow during the dissipation process [29]. Therefore, time-dependent behavior and drainage conditions are ignored in this study. To simplify the calculation, the following assumptions are adopted:

(1) The soils are assumed to be ideally elastic materials, and the tunneling-induced movements are considered as plane strain problem

(2) The tunnel opening is perfectly a circle, and the movement focus of soils is exactly the tunnel center

(3) The soil is in close contact with the liner, and the distortion of liner causes no ground loss, and the thickness of liner is assumed to be zero

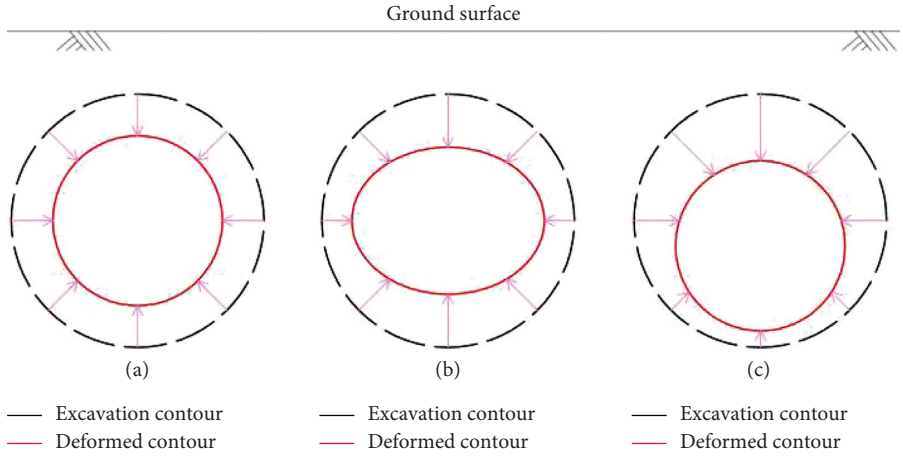

Figure 1: Convergence patterns at the tunnel opening. (a) Uniform radial pattern. (b) Oval-shaped pattern. (c) Nonuniform radial pattern.

2.2. Convergence Deformation Patterns around Tunnel Opening. The ground movements around the tunnel opening are solved as the combination of three fundamental deformation modes, as shown in Figure 2, with input parameters, u_0, u_v, and u_e, corresponding to uniform convergence, vertical translation, and ovalization, respectively. Among them, the components u_v and u_e reflect the nonuniform convergence deformation.

2.3. Derivation of Expression for Generalized Displacement Boundary Condition. The generalized displacement boundary refers to the displacement of soils along the circumference in the radial direction. The analysis model of generalized displacement boundary is illustrated in Figure 3, where rectangular coordinate and polar coordinate with the same origin are established, respectively. Based on the basic assumption and convergence deformation pattern above, the radial displacement U_0 along the circumference using polar coordinate can be expressed as

$$U_0 = -[R + u_0 - \rho(\theta)], \tag{1}$$

where R and u_0 are tunnel radius and uniform convergence, respectively, and $\rho(\theta)$ refers to the transverse curve of liner, which can be expressed by an elliptic equation:

$$\frac{x^2}{a^2} + \frac{(y+c)^2}{b^2} = 1, \tag{2}$$

where $a = R + u_e$, $b = R - u_e$, and $c = u_v$.

While in rectangular coordinate, the curve of liner can be obtained as

$$\rho(\theta) = \frac{-a^2 c \sin\theta + ab\sqrt{a^2\sin^2\theta + (b^2 - c^2)\cos^2\theta}}{b^2\cos^2\theta + a^2\sin^2\theta}. \tag{3}$$

By substituting equation (3) into equation (1), then the expression for generalized displacement boundary condition is obtained.

3. Analytical Solution for Ground Movements Based on Generalized Displacement Boundary

3.1. Analytical Model and Boundary Conditions. The initial stress state of soil depends on the analysis model of tunnel excavation, which covers three types, as shown in Figure 4. The major difference between the three models is the stress state far from the tunnel opening. The first model (Figure 4(a)) assumes that uniform pressure is exerted around the plane edge [44, 45], which conforms with the practical condition, while the lateral pressure coefficient is considered in the second case [28], as shown in Figure 4(b), which is relatively consistent with the practical condition. The third further introduces the tunnel depth and radius [29, 30], as shown in Figure 4(c), which can better estimate the soil stress of shallow buried tunnel, but otherwise may lead to complicated analytical solution or even violated physical laws in some cases. Therefore, the second analytical model is chosen in this study.

The Airy stress function can be assessed by dividing the applied stresses into isotropic and deviatoric parts [28–30]:

$$\varphi = \frac{p}{2}r^2 + \frac{q}{2}r^2\cos 2\theta, \tag{4}$$

where $p = ((\sigma_v + \sigma_h)/2) = -((1+k)\gamma h/2)$, $q = ((\sigma_v - \sigma_h)/2) = -(((1-k)\gamma h)/2)$, and σ_v and σ_h are the vertical and horizontal stress, respectively.

It is noted that the axial stress is ignored in the above definitions for deviator and mean effective stresses. Sheng et al. [46] stated that the errors due to the simplified definitions are negligible. Based on the relationship between Airy stress function and stresses [47], the stresses in the initial field can be derived as

$$\begin{cases} \sigma_{r0} = -\dfrac{1+k}{2}\gamma h + \dfrac{1-k}{2}\gamma h\cos 2\theta, \\ \sigma_{\theta 0} = -\dfrac{1+k}{2}\gamma h - \dfrac{1-k}{2}\gamma h\cos 2\theta, \\ \tau_0 = -\dfrac{1-k}{2}\gamma h\sin 2\theta. \end{cases} \tag{5}$$

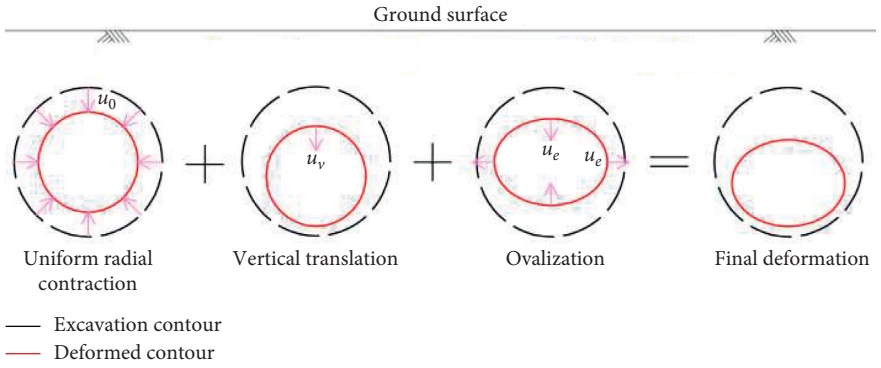

Figure 2: Convergence deformation pattern around tunnel opening in this study.

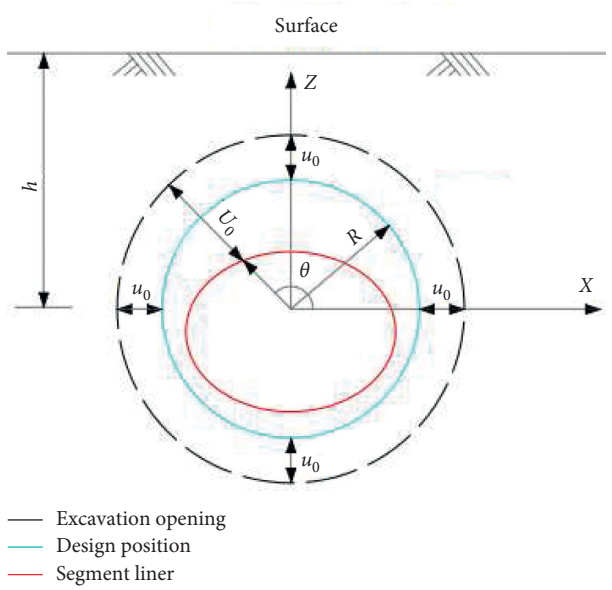

Figure 3: Analysis model of generalized displacement boundary.

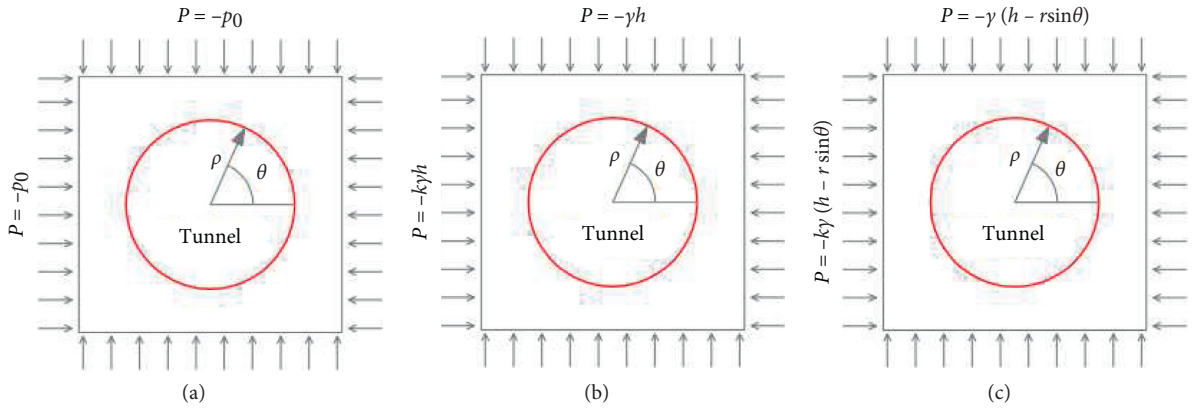

Figure 4: Analysis model for tunnel excavation.

The boundary conditions far from and around the tunnel opening can be obtained, respectively, as

$$\begin{cases} \sigma_r|_{r \longrightarrow \infty} = \sigma_{r0}, \\ \sigma_\theta|_{r \longrightarrow \infty} = \sigma_{\theta 0}, \end{cases} \tag{6}$$

$$\begin{cases} \sigma_r|_{r=R} = \tau|_{r=R} = 0, \\ U_r|_{r=R} = U_0, \\ U_\theta|_{r=R,\theta=\pm(\pi/2)} = 0, \end{cases} \tag{7}$$

where equation (7) is the generalized displacement boundary condition originally introduced in this paper.

3.2. Analytical Prediction for Ground Movement. Using the coordinate system shown in Figure 3, Park [28] simplified the Airy stress function introduced by Timoshenko and Goodier [48] and obtained a general solution for the tunnel excavation problem. Substituting equations (6) and (7) into the general solution presented by Park [28], the analytical formula, which is able to compute tunneling-induced ground movements basing on generalized displacement boundary condition, can be obtained as

$$\begin{cases} U_r = \dfrac{1}{2G}\left\{-a_0 r^{-1} + 2\left[a_2' r^{-3} - 2(1-\nu) b_2' r^{-1}\right]\cos 2\theta\right\}, \\ U_\theta = \dfrac{1}{2G}\left[a_2' r^{-3} - (1-2\nu) b_2' r^{-1}\right]\sin 2\theta, \end{cases} \tag{8}$$

where $a_0 = 2Ga(R + u_0 + ((a^2 c \sin\theta - ab\sqrt{a^2\sin^2\theta + (b^2 - c^2)}\cos^2\theta)/(b^2\cos^2\theta + a^2\sin^2\theta)))$, $a_2' = -((1-k)/4)\gamma h a^4$, and $b_2' = ((1-k)/2)\gamma h a^2$.

Further, the ground surface and subsurface settlements U_z and the lateral deformation U_x can be estimated as follows:

$$\begin{cases} U_x = -U_r \cos\theta + U_\theta \sin\theta, \\ U_z = -U_r \sin\theta - U_\theta \cos\theta, \end{cases} \tag{9}$$

where $r = \sqrt{x^2 + y^2}$, $\sin\theta = (y/r)$, and $\cos\theta = (x/r)$.

Compared with available analytical solutions (Park [28]; Tong et al. [30]; Zhang et al. [29]), due to inclusion of the term $\ln r$, equations (8) and (9) need no mathematical corrections; consequently, it eliminates the resultant errors.

4. Estimation of the Characteristic Parameter of the Generalized Displacement Boundary

As mentioned above, the ground movements around the tunnel opening are considered as a combination of three basic modes, namely, uniform convergence u_0, vertical translation u_v, and ovalization u_e. Therefore, in order to accurately assess the analytical solution presented in Section 3, the characteristic parameter (u_0, u_v, u_e) of these three modes must be first estimated. Unfortunately, rather few data on vertical translation and ovalization of tunnel are currently available [39], which mostly are estimated empirically [31, 49] or by contrast analysis with several groups of prescribed displacement [28–30]. So these parameters are subjective and thus have limited applicability. In fact, the characteristic parameters u_v and u_e are related to numerous factors, such as geological conditions and construction technique [40]. A slight change in engineering conditions may produce significant effects in the degree of u_v and u_e.

4.1. Uniform Radial Convergence Parameter u_0. The uniform radial convergence u_0 can be estimated with respect to the volume loss as shown in

$$u_0 = \frac{RV_l}{2}, \tag{10}$$

where R is tunnel radius and V_l is volume loss, which can be estimated based on the gap parameter introduced by Lee et al. [43].

4.2. Nonuniform Convergence Parameter (u_v, u_e). In order to associate the nonuniform convergence parameter with engineering conditions and facilitate engineering application, u_v and u_e are expressed as multiples of the uniform radial convergence parameter u_0 in this study as shown in

$$\begin{cases} u_v = mu_0, \\ u_e = nu_0, \end{cases} \tag{11}$$

where $m \in [0, 1]$, $n \in [0, \infty)$. $m = 0$ and $n = 0$ refer to only uniform radial convergence, as shown in Figure 1(a), while $m = 0$, $n \neq 0$ indicate that only ovalization occurs, as shown in Figure 1(b); $m \neq 0$ and $n = 0$ suggest convergence patterns as shown in Figure 1(c), with only vertical translation.

Table 1 presents the engineering information of the 20 case studies previously investigated by various authors. The optimal value of m and n in equation (11) can be obtained by applying the least square method to equation (9). Based on the observed data and the resulting solution, Figure 5 is prepared with the distance from center line of tunnel as the horizontal coordinate, and the surface settlement as the vertical coordinate, while the optimal m and n are plotted against the dimensionless h/R ratio in Figure 6. It can be seen that none of the parameters shows a tendency to vary with the relative depth h/R. Note that the optimal m are concentrated around 0, 0.5, and 1, which coincide well with the research findings reported by Bobet [37], Zhang et al. [29], Tong et al. [30], and Jiang and Zhao [49].

4.2.1. The Ovalization Coefficient n. The effect of the tunnel ovalization can be further quantified by the dimensionless distortion coefficient with respect to u_e and R as shown in

$$\delta = \frac{u_e}{R}. \tag{12}$$

Based on the 20 case studies listed in Table 1 and the corresponding optical m, Figure 7 shows the relationship between the dimensionless distortion coefficient and the volume loss. It can be seen that the relative ovalization coefficient increases overall linearly with the volume loss. Therefore, in this study, the relationship between the

Table 1: Cases of surface settlement induced by shield tunneling.

Case no.	$m = 0$ (m)	$Z_{m=i}$ (kPa)	$m = i \in (0, 1]$	$Z_{m=i} = a_i Z_0$ (mm)	Soil	References
1	10.7/2.47	104	—	164	Soft clay	Palmer and Belshaw [50]
2	19.0/8.5	3.5×104	—	58	Clay	Deane and Bassett [51]
3	18.5/2.66	3.5×104	—	81	Clay	Phienwej [52]
4	29.4/4.14	45×104	—	34	Soft clay	Attewell and Farmer [53]
5	10.0/8.0	2.55×104	—	31	Clay	Ledesma and Romero [54]
6	29.83/11.65	1.745×104	—	53.5	Clay	Lin et al. [55]
7	15/6.2	2.05×104	0.33	36.5	Soft clay	Lee et al. [56]
8	15.88/7.48	2.05×104	—	60	Sandy silt	Zhang et al. [57]
9	14/13.95	0.355×104	0.28	47.1	Silty clay	Xie et al. [58]
10	14/13.95			33.2		
11	14/13.95			17.5		
12	19/6.2	—	—	34.1	Silty	Chen et al. [59]
13	19/6.2			26.8	Silty	
14	17.7/8.43	11.85×104	0.3	7.4	Sandy clay	Maynar and Rodriguez [60]
15	8.5/12.68	1.35×104	0.41	12	Silty clay	Shi et al. [28]
16	19/5.49	—	—	98.3	Soft clay	Rowe and Kack [42]
17	11.7/2.82	0.45×104	—	429.7	Soft clay	
18	14/6.5	—	—	54.6	Stiff clay	
19	11.85/6.39	—	—	39	Silty clay	Zeng et al. [61]
20	20.055/6.2	—	—	17.7	Silty clay	Zhang and Yan [62]

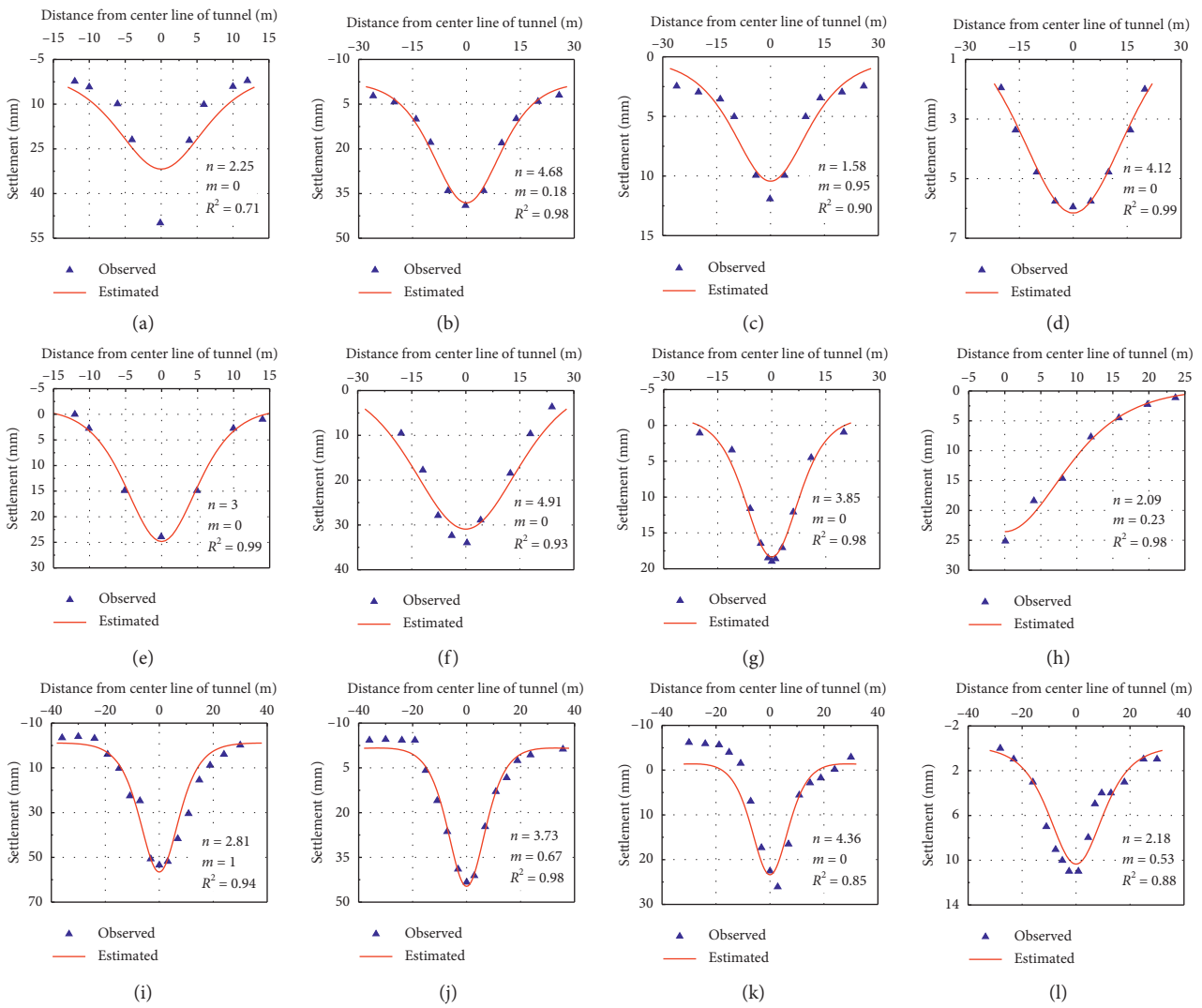

Figure 5: Continued.

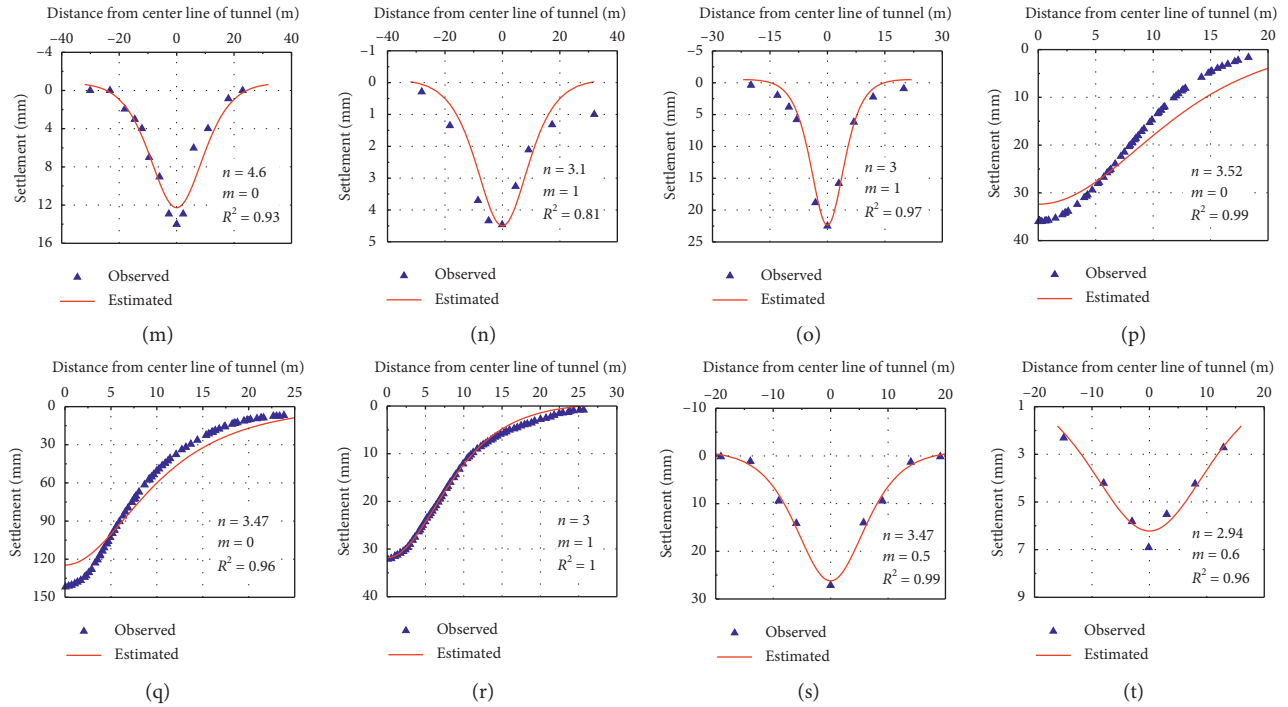

FIGURE 5: Measured surface settlements vs computed surface settlements. (a) Case 1, (b) Case 2, (c) Case 3, (d) Case 4, (e) Case 5, (f) Case 6, (g) Case 7, (h) Case 8, (i) Case 9, (j) Case 10, (k) Case 11, (l) Case 12, (m) Case 13, (n) Case 14, (o) Case 15, (p) Case 16, (q) Case 17, (r) Case 18, (s) Case 19, and (t) Case 20.

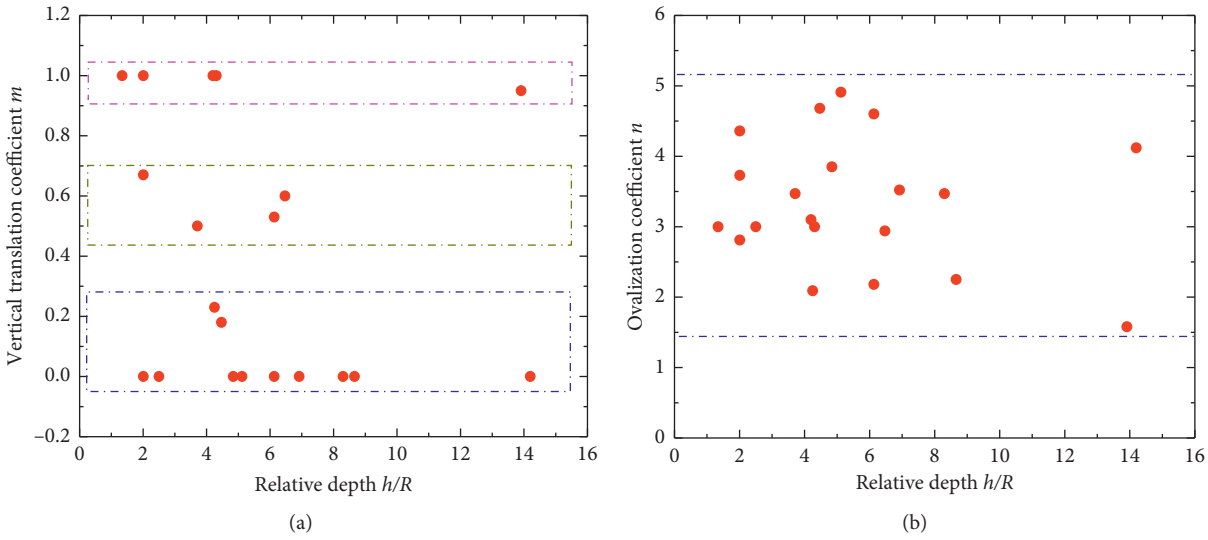

FIGURE 6: Summary of fitted nonuniform convergence parameters. (a) Vertical translation coefficient m. (b) Ovalization coefficient n.

dimensionless distortion coefficient and volume loss is written as

$$\delta = 1.365\, V_l + 0.0027. \tag{13}$$

In the absence of measured tunnel ovalization, by combining equations (10)–(13), an empirical method for estimating the tunnel ovalization can be obtained as shown in the following:

$$n = 2.73 + \frac{0.0054}{V_l}, \tag{14}$$

$$u_e = 1.365\, V_l R + 0.0027R. \tag{15}$$

For many cases of tunneling in soft ground, the typical volume losses are generally around 1% under well controlled conditions [63], while they may be within 0.1–0.5 % by

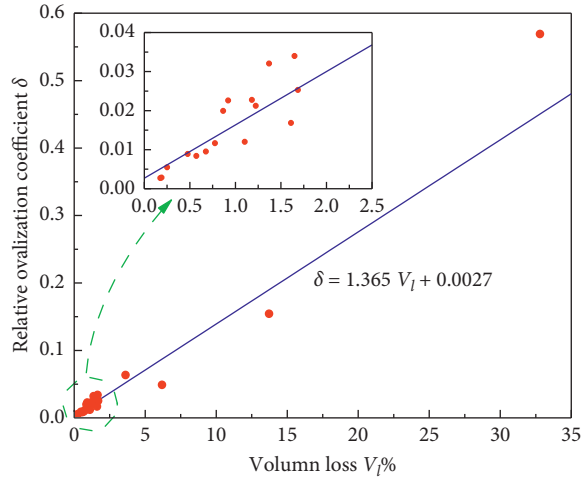

Figure 7: Relationship between relative ovalization coefficient and volume loss.

taking special measures [64]. Figure 7 indicates that a good agreement can be found from equation (13) when the volume loss is under 1%. Therefore, the tunnel ovalization parameter can be rationally estimated by equation (14) in most cases.

4.2.2. The Vertical Translation Coefficient m. The transverse settlement curve is characterized by the maximum settlement and the trough width parameter. In this study, taking the maximum settlement Z_0 where $m = 0$ as a reference, the maximum settlement $Z_{m=i}$ at $m = i \in (0, 1]$ is defined as

$$Z_{m=i} = a_i Z_0. \tag{16}$$

Similarly, based on C_0 where $m = 0$, the trough width parameter $C_{m=i}$ at $m = i \in (0, 1]$ is defined as

$$C_{m=i} = b_i C_0, \tag{17}$$

where the coefficients a_i and b_i are greater than zero. The greater the a_i, the larger the maximum settlement; and the greater the b_i, the wider the trough width parameter.

Figure 6 shows that the coefficient m is concentrated around 0, 0.5, and 1. Therefore $i = 0.5$ and $i = 1$ are selected as an example for further analysis in this section. Figures 8 and 9 show the relationship between the coefficients a_i,b_i and the nonuniform convergence coefficient m, n, the gap parameter g, the tunnel depth h, and the tunnel radius R, respectively. The following findings are found:

(1)The coefficient a_i is independent of the gap parameter, the depth, and the radius, while it is positively and negatively related to the coefficients m and n, respectively. The coefficient$n$ can be estimated within 3.27~8.17 from equation (14) for most cases of tunneling where typical volume losses are within 0.1–1%. According to Figure 8(c), for most tunnel projects, the ratio of $Z_{m=i}$ and Z_0 falls in the quadrilateral cdef, with the maximum ratio of 1.23; that is, the maximum settlement is only 23% higher than the reference in the most unfavorable case.

(2) It is noted that the change of the gap parameter, the depth, and the radius produced negligible effects on the degree of the coefficient b_i, where no more than 1% can be observed. Therefore, it can be considered that the coefficient b_i has no relation with the above parameter. Similarly, it is positively and negatively related to the coefficients$m$ and n. Figure 9(c) indicates that, for most tunnel projects, the ratio of $C_{m=i}$ and C_0 falls in the quadrilateral ghij, with the maximum ratio of 1.082; that is, the trough width parameter is only 8.2% higher than the reference in the most unfavorable case.

To sum up, the nonuniform convergence coefficient m is assumed to be 0 when estimating the tunneling-induced ground movement by the method presented in this paper. The final result can be obtained increasing by 0–23%, depending on construction conditions. For example, the increase by 0% may be adopted when taking special measures, while the increase by 23% may be adopted under poor grouting quality, where the result is relatively conservative so as to ensure the safety.

5. Model Validation

5.1. Comparisons with Field Data. Tunnel excavation would inevitably cause vertical and horizontal ground movements. Tables 1–3 summarize the engineering information of previous various case studies concerning surface settlement, underground settlement, and horizontal displacement, respectively. Based on the case studies listed in Tables 1–3, we compare the analytical prediction with the same kind of other methods presented by [28–30] and then check the reliability and applicability of the proposed solutions in this paper. It should be noted that the above three other methods adopt the same deformation pattern as in this paper, but impose different displacement boundary condition, and their nonuniform convergence parameters are empirically prescribed.

(1) Surface settlement: comparison of analytical surface settlements and field observation is presented in Figure 10. Only some results of cases listed in Table 1

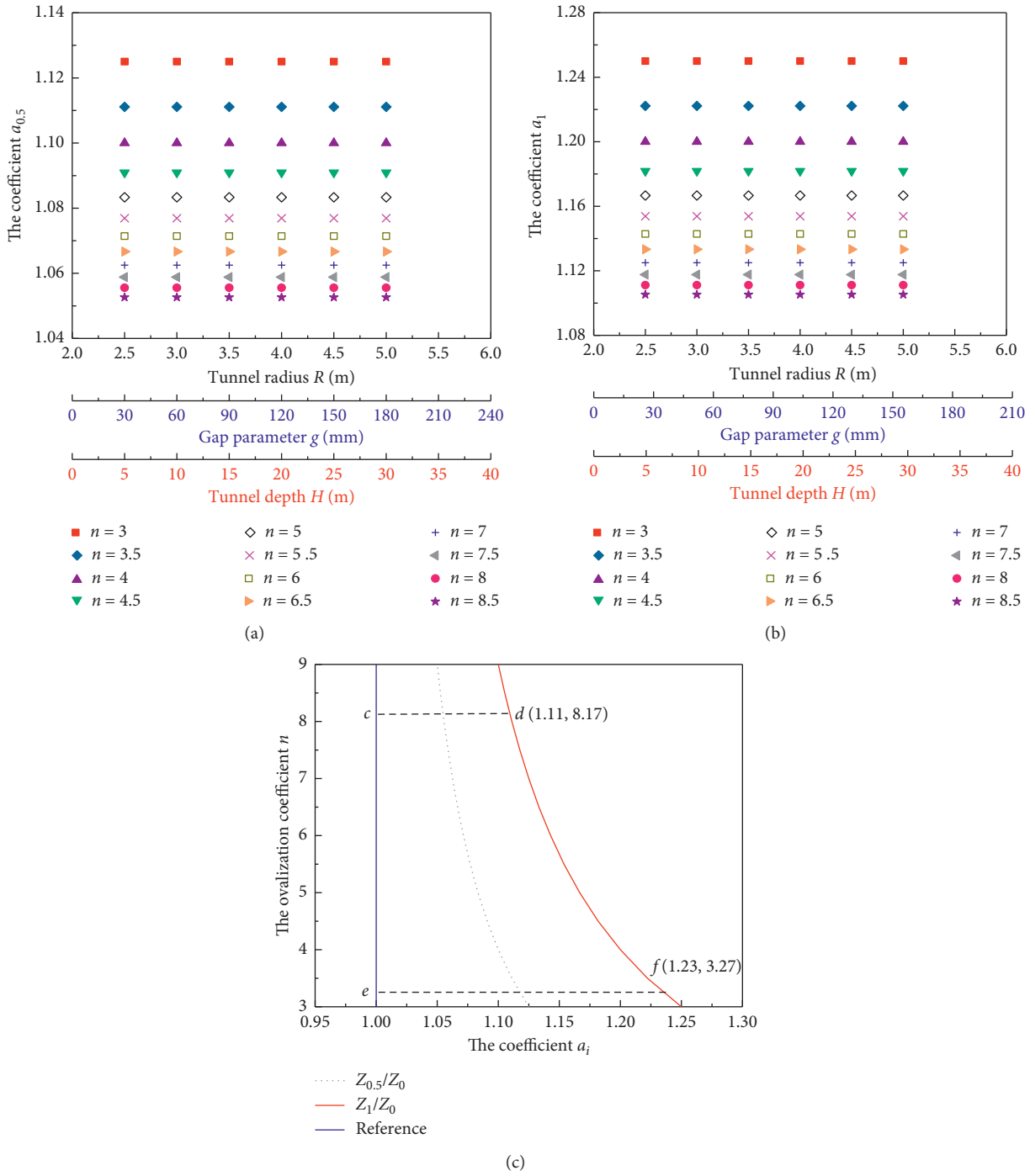

Figure 8: Relationship between αi and m, n, g, h, and R. (a) $m = 0.5$. (b) $m = 1$. (c) Relationship between αi and m, n.

are selected as examples to illustrate the reliability and applicability of the proposed solutions. From Figure 10, the following can be seen:

(1) Generally, the surface settlements estimated by the analytical method in this paper agree well with the field observations. As for some cases, such as cases 18 and 19, the results increasing by 23% is preferable, for the segment liner to sink to the bottom of excavation opening due to not timely filling into the gap between tunnel opening and liner.

(2) The methods proposed by Park [28], Tong et al. [30], and Zhang et al. [29] all have the risk of seriously overestimating the maximum settlement and underestimating the trough width, as shown in cases 18 and 19. The main reason may be that their displacement boundary condition is unable to fully reflect the convergence patterns

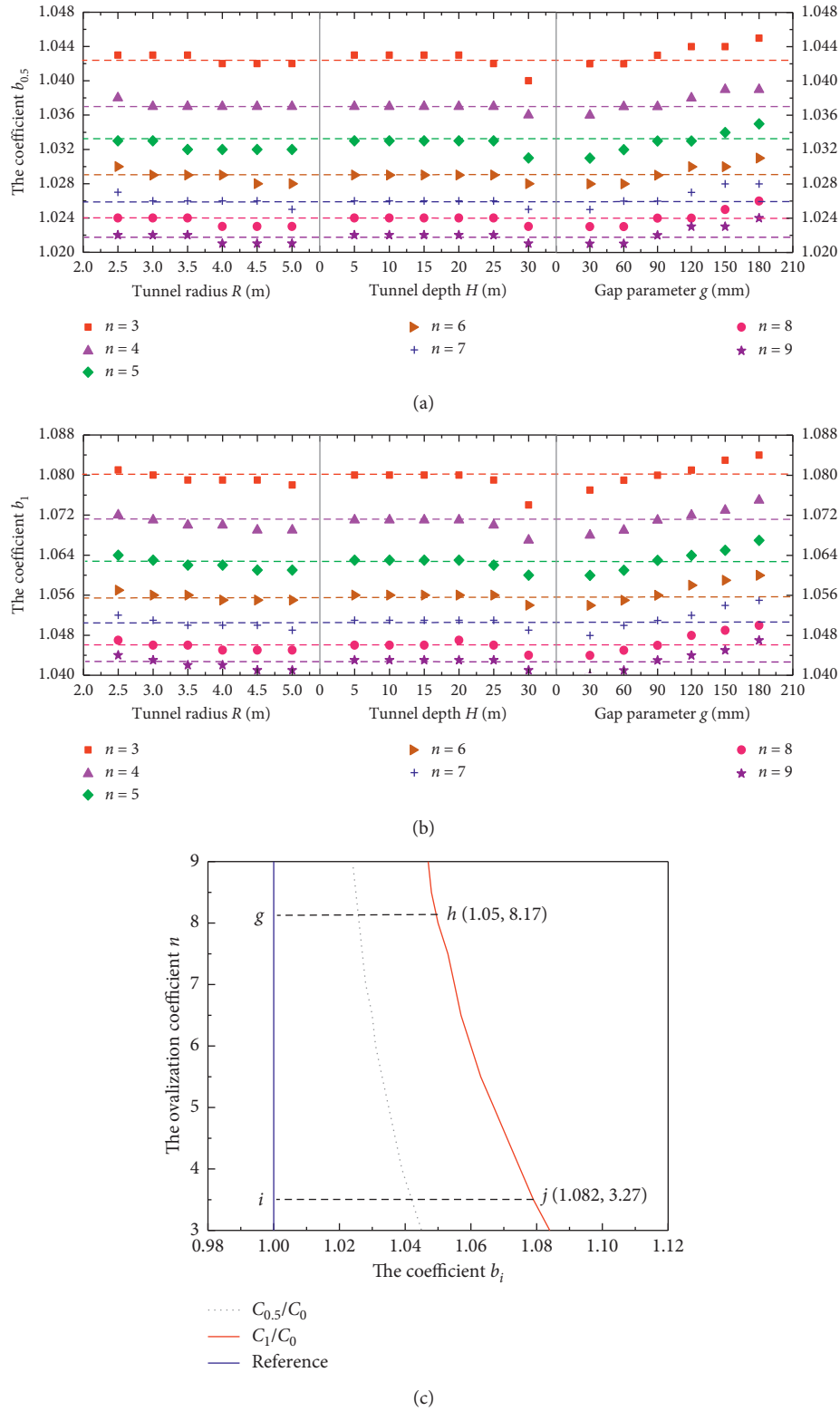

Figure 9: Relationship between bi and m, n, g, h, and R. (a) $m = 0.5$. (b) $m = 1$. (c) Relationship between bi and m, n.

around the tunnel opening. Besides, the corresponding nonuniform convergence parameters are fixed values estimated empirically. In other word, their displacement boundary conditions do not vary with the engineering conditions, and therefore they are only applicable to the prediction of ground movements in specific projects. In addition, it is worth noting that the

Table 2: Cases of underground settlement induced by shield tunneling.

Case no.	g (m)	g (kPa)	H	R(mm)	Soil	References
1	5.6/4.2	—	—	79.9	Clay	Yi et al. [67]
2	9.0/4.0	—	—	350.1	Clay	Fang and Chen [66]
3	19.0/6.2	—	—	29.2	Clay	Fang et al. [15]; Chen et al. [59]

Note: the value of $g$is obtained by inversion with respect to the maximum surface settlement.

Table 3: Cases of horizontal displacement induced by shield tunneling.

Case no.	H (m)	R (kPa)	g	H(mm)	Soil	References
1	10.7/2.47	104	—	164	Soft clay	Palmer and Belshaw [50]
2	18.5/2.66	3.5×104	—	81	Clay	Phienwej [52]
3	19.0/8.5	3.5×104	—	58	Clay	Deane and Bassett [51]
4	11.848/6.2	—	—	110	Clay	Jiang et al. [67]

The value of $R$is obtained by inversion with respect to the maximum surface settlement.

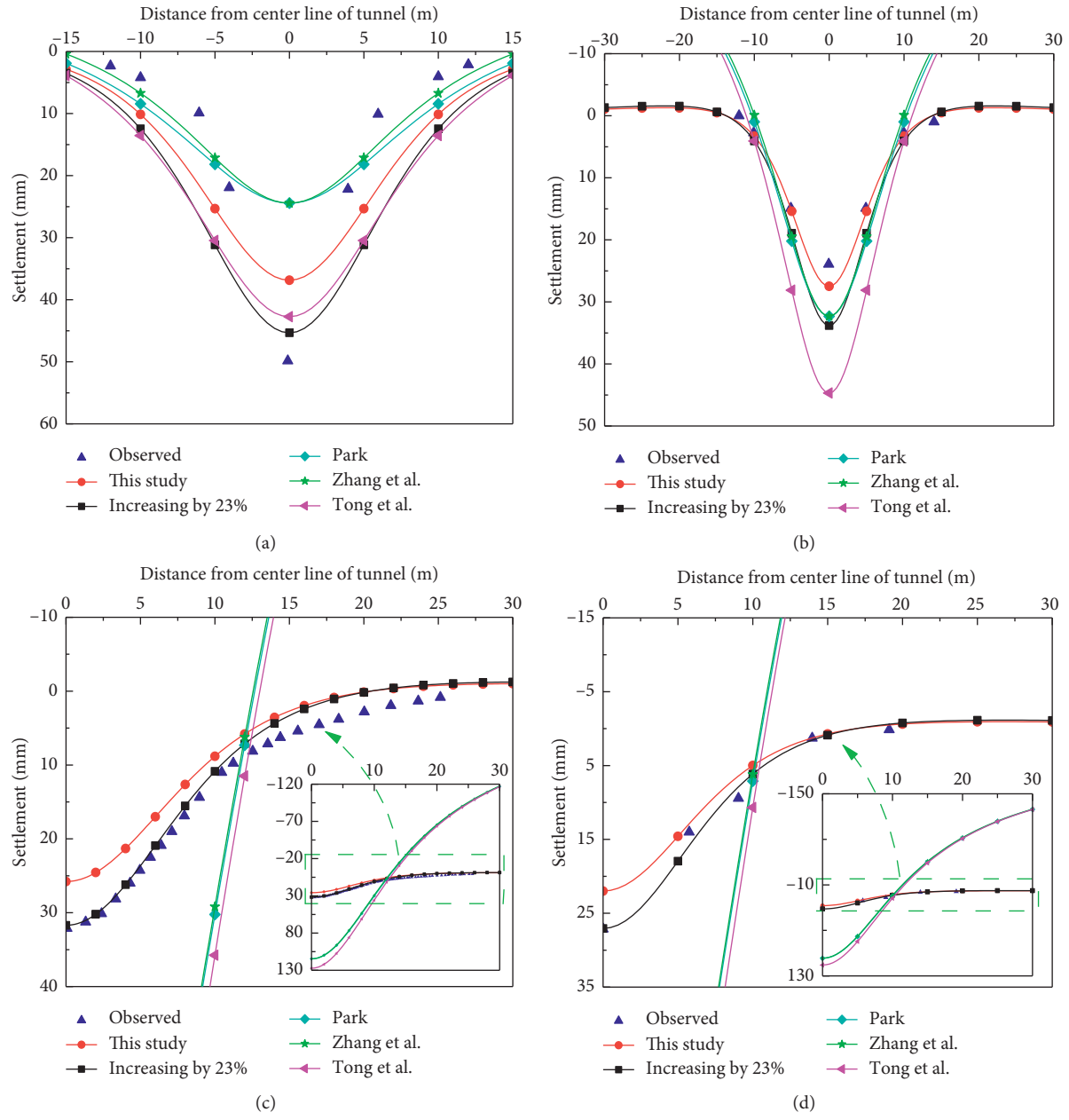

Figure 10: Comparison of analytical surface settlements and field observation. (a) Case 1: Thunder Bay Tunnel. (b) Case 3: Barcelona Tunnel. (c) Case 18: Frankfurt Subway. (d) Case 19: Line 1 of Tianjing Metro.

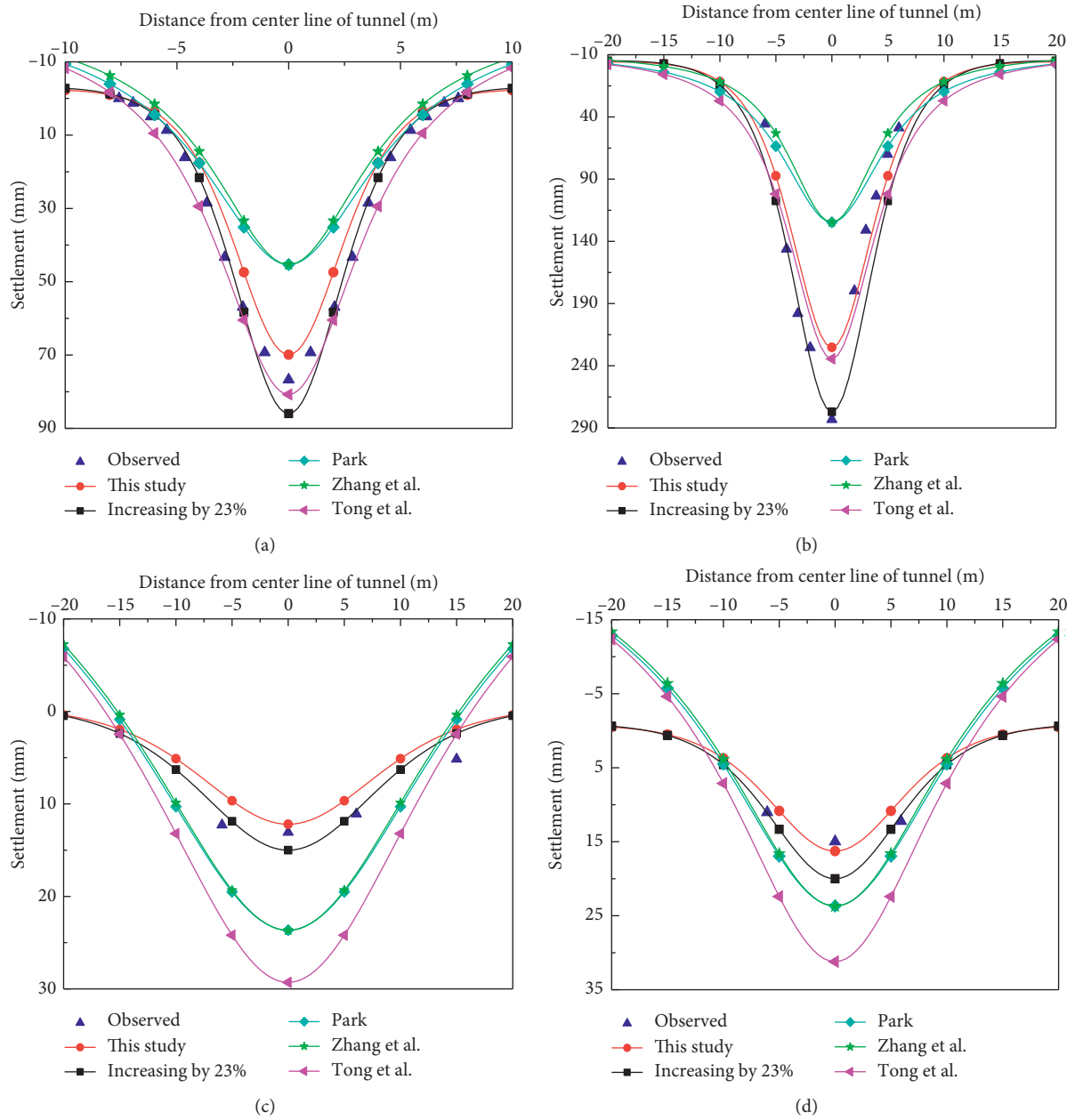

Figure 11: Comparison of analytical underground settlements and field observation. (a) Case 1: Furongjiang Sewer. (b) Case 2: Taipei Sewerage Section 1. (c) Case 3: Hangzhou Metro, Right Line. (d) Case 4: Hangzhou Metro, Right Line.

settlement curves of Park's method and Zhang's method are almost identical trough imposing different displacement boundary condition. And the predicted curve of Tong is highly consistent with Park's method and Zhang's method for the project shown in Figures 10(c)–10(d), which indicates their difference in displacement boundary conditions is offset by other factors.

(2) Underground settlement: comparison of analytical underground settlements and field observation is shown in Figure 11. To illustrate the applicability of the proposed method in this paper, results at different depths are compared. Figures 11(a)–11(d) present results at depths of 0.91 m, 2.9 m, 3.0 m, and 7.0 m, respectively. The following findings are found:

(1) Compared with other method, the underground settlements calculated by the proposed method in this paper are more reasonable. Similarly, the results increasing by 23% is preferable for some cases as shown in Figures 11(b)–11(d).

(2) As the same with the law of surface settlements, the curves of underground subsidence by Park's method and Zhang's method are also highly similar, and their maximum values are often

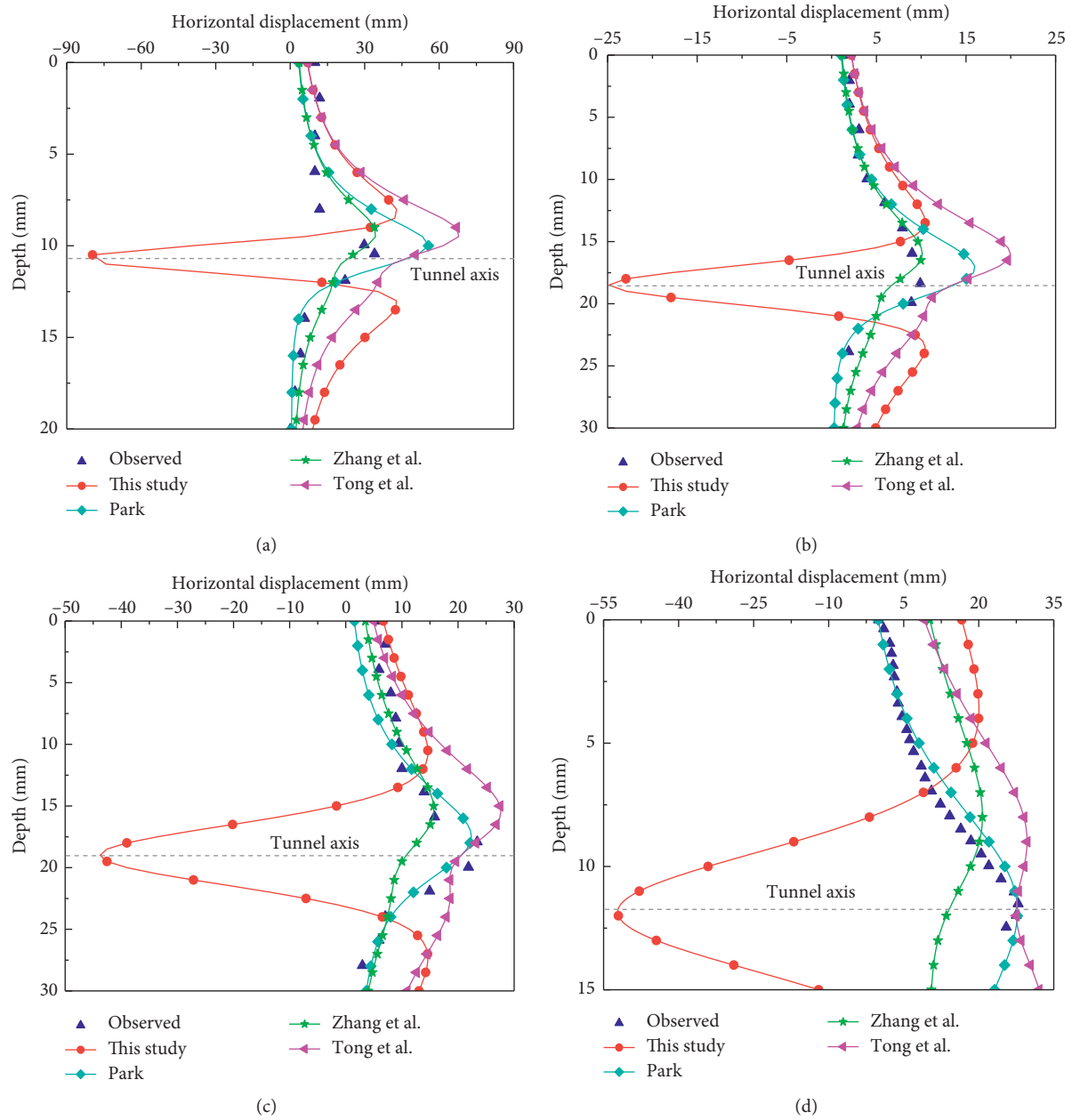

Figure 12: Comparison of analytical horizontal displacements and field observation. (a) Case 1: Thunder Bay Tunnel. (b) Case 2: Bangkok Sewer Tunnel. (c) Case 3: Heathrow Express Trial Tunnel. (d) Case 4: Line 1 of Tianjing Metro Section 1.

smaller than the observed value. Comparatively speaking, Tong's method is also considerably reliable in the prediction of underground subsidence. It can be noted that Tong's method always predicted a larger value than Park's method and Zhang's method, because Tong's method doubled the value of characteristic parameters.

(3) Horizontal displacement: comparison of analytical horizontal displacements and field observation is shown in Figure 12. To illustrate the applicability of the proposed method in this paper, results at different horizontal distance from the center line of tunnel are compared. Figures 12(a)–12(d) present results at horizontal distance of 2.2 m, 4.0 m, 6.0 m, and 6.2 m, respectively. It should be noted that the movement of soil towards the tunnel is positive. Unfortunately, an uncommon phenomenon appears where the horizontal displacement obtained by the proposed method is negative around tunnel depth; this is because the ovalization parameter obtained by the proposed empirical formula is so large that the soils at the excavation opening move back to the center of tunnel within a certain angle of the opening, thus squeezing the surrounding soils. In

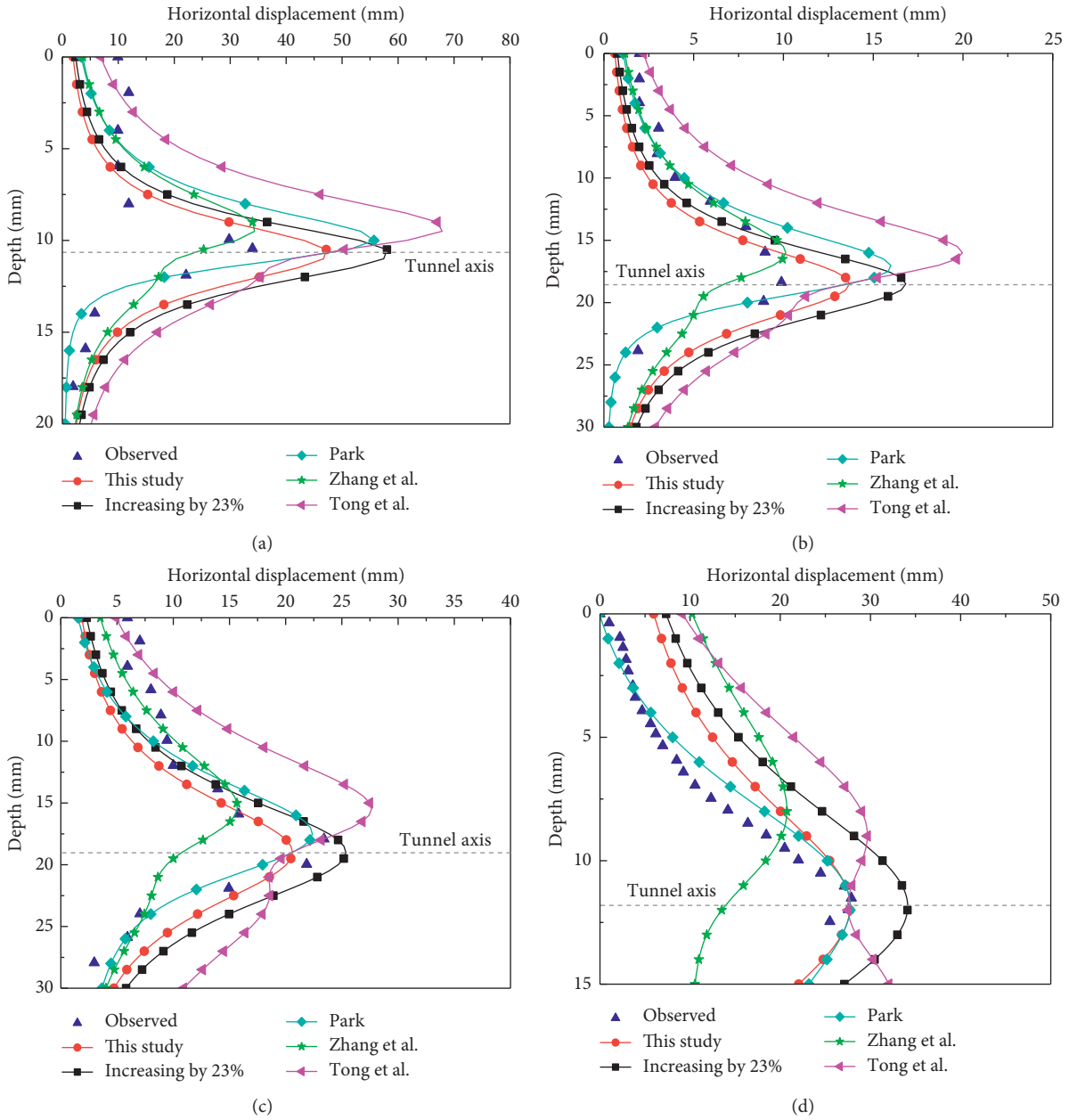

Figure 13: Comparison of analytical horizontal displacements and field observation. (a) Case 1: Thunder Bay Tunnel. (b) Case 2: Bangkok Sewer Tunnel. (c) Case 3: Heathrow Express Trial Tunnel. (d) Case 4: Line 1 of Tianjing Metro Section 1.

order to eliminate this uncommon phenomenon, it is suggested to ignore the influence of ovalization when predicting the horizontal displacement proposed in this paper. It is worth noting that this special approach has no theoretical support but is based on empirical analysis. Figure 13 presents comparison of analytical horizontal displacement and field observation when ovalization is neglected by the proposed method. The following can be seen:

(1) The horizontal displacement calculated by the proposed method in this paper is reasonable. It can be noted that the position of maximum horizontal displacement obtained by the method in this paper is always close to the tunnel axis, which is quite consistent with the practical condition.

(2) The horizontal displacement predicted by Park's method is also reliable. Unlike the similarity of settlement curve, the horizontal displacement curves of Park's method and Zhang's method do not coincide, which indicates that their difference of boundary conditions has a prominent influence on predicting for horizontal displacement. The maximum horizontal displacement obtained by Tong's method is always relatively large.

The influence of ovalization is neglected in the proposed method .

Table 4: Gap parameter of six cases.

Case	g(mm)	H(m)	R(m)
1	30	10	3
2	60	10	3
3	90	10	3
4	120	10	3
5	150	10	3
6	180	10	3

Table 5: Tunnel depth of six cases.

Case	g(mm)	H(m)	R(m)
1	90	5	3
2	90	10	3
3	90	15	3
4	90	20	3
5	90	25	3
6	90	30	3

5.2. Parametric Analyses. The primary parameters, including the tunnel geometry, the tunnel depth, and the gap parameter, have a significant influence on the ground settlements. The influence of those parameters on the ground settlements was investigated by parametric analyses in terms of the maximum settlement and the trough width parameter. The following basic parameters are set: the soil elastic modulus, $E = 2.5 \times 10^4$ kPa, the soil Poisson's ratio, $\nu = 0.5$, the soil lateral pressure coefficient, $k = 1$, the calculated position of settlement,z = 0 m, namely, surface settlement. The analysis cases are summarized in Tables 4–6 . And the related results are shown in Figures 14–16 , respectively. The parametric analysis demonstrates the following:

(1) The maximum settlement increases linearly with the gap parameter and the tunnel radius. This is because the ground movements are related to the deformation around the opening, and the larger the gap parameter and the larger the radius, the larger the displacement at the excavation surface, while the maximum settlement is negatively related to the tunnel depth. Due to the limited scope of stress unloading caused by tunnel excavation, the greater the depth, the less the impact on the surface settlement. It should be noted that when the depth is more than 20 m, the increase of this parameter slightly affects the maximum surface settlement.

(2) The trough width parameter increases linearly with the gap parameter and the tunnel depth, while being negatively related to the tunnel radius. However, further analysis indicates that when the gap parameter increases by 2 times, the trough width parameter only increases by 1.35%, and when the radius increases by 1 time, the trough width parameter only increases by 0.47%. Therefore, it can be considered that the trough width parameter is independent of the gap parameter and the radius.

(3) To date, various expressions have been proposed for estimating the trough width parameter$i$. Generally, they could be divided into three categories: (1) i is regarded as a function of the friction angle of soil ϕ and tunnel depth H, namely, $i = f(\phi, H)$ [11]; (2) i is related to the tunnel radius R and tunnel depth H in the form of $i = Ra(H/2R)^n$ or $i = a(bH + cR)$ [68]; (3) i depends only on the tunnel depth H with $i = aH + b$ [69]. The parameters a, b, c, n are all pending constants fitted from field observation. According to the above findings, this paper considers that the third kind is more reasonable and suggests $i = 0.66H + 0.45$.

Table 6: Tunnel radius of six cases.

Case	g (mm)	H (m)	R (m)
1	90	10	2.5
2	90	10	3
3	90	10	3.5
4	90	10	4
5	90	10	4.5
6	90	10	5

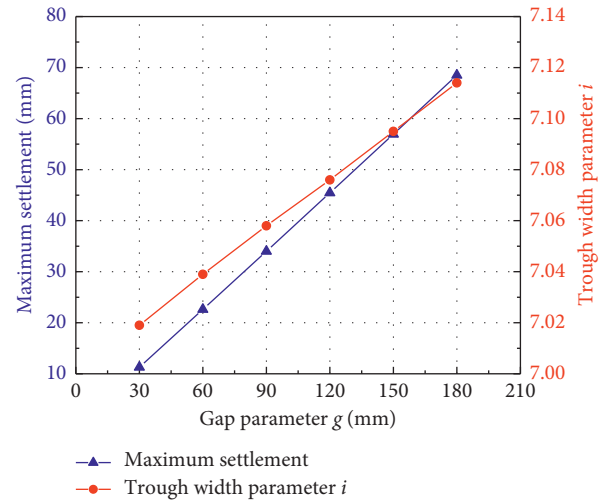

Figure 14: Effect of gap parameter on settlement.

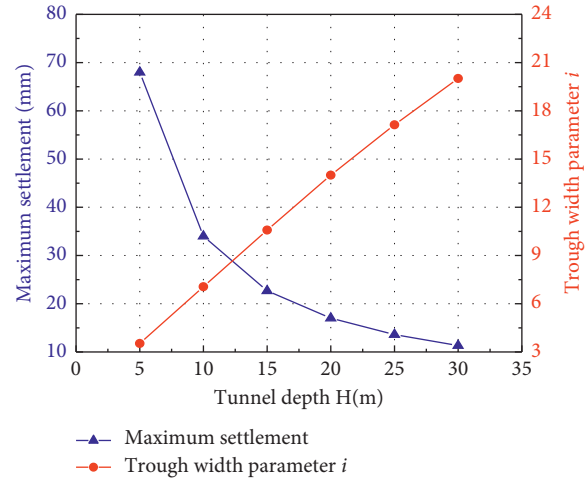

Figure 15: Effect of tunnel depth on settlement.

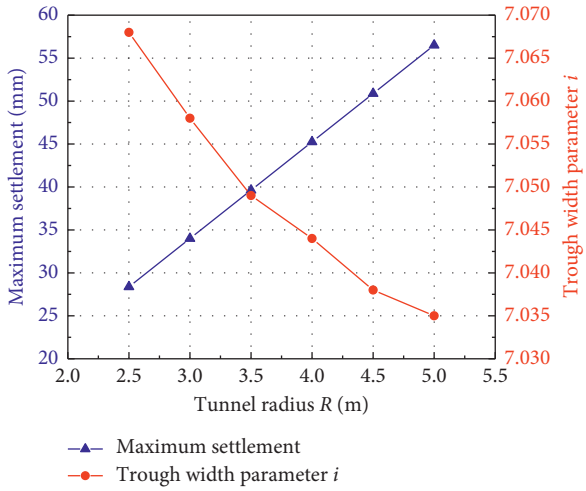

Figure 16: Effect of tunnel radius on settlement.

6. Conclusion

In this study, the convergence deformation around tunnel opening is summarized, and then a universal pattern of displacement boundary condition around the tunnel cavity is originally introduced, which is solved as the combination of three fundamental deformation modes, namely, uniform convergence, vertical translation, and ovalization. The expression for the above-mentioned displacement boundary condition is derived and the stress boundary is obtained based on an optimal plane analysis model, by imposing which, the analytical solution for ground movements, based on the stress function method, is proposed.

(1) The analytical method is validated against a set of 20 field cases with monitoring data, based on which, the nonuniform convergence parameters of the generalized displacement boundary are summarized and then the empirical methods estimating the nonuniform convergence parameters are obtained as follows: ovalization parameter $u_e = 1.365V_lR + 0.0027R$; vertical translation parameter $u_v = 0u_0$, and the final result can be obtained increasing by 0~23%, depending on construction details.

(2) The reliability and applicability of this proposed solution are verified by comparing the observed data in terms of surface settlement, underground settlement, and horizontal displacement. For some cases, the available predicted methods based on the stress method all have the risk of seriously overestimating the maximum settlement and underestimating the trough width. The difference in boundary conditions between Park's method and Zhang's method has little influence on predicting surface settlement but has obvious effect on the horizontal displacement. Among them, Tong's method always predicted a larger value.

(3) Further parametric analyses indicated the following: (1) the maximum settlement increases linearly with the gap parameter and the tunnel radius, while it is negatively related to the tunnel depth and it should be noted that when the depth is more than 20 m, the increase of this parameter slightly affects the maximum surface settlement. (2) The trough width parameter is independent of the gap parameter and the radius, while it is proportional to the tunnel depth and it suggests $i = 0.66H + 0.45$.

Data Availability

All data are included within the article.

Conflicts of Interest

The authors declare that they have no conflicts of interest.

Acknowledgments

Funding for this paper by the National Natural Science Foundation of China (Nos. 51978669 and U1734208) and Innovation-Driven Project of Central South University (No. 2020CX011) is gratefully acknowledged.

References

[1] M. Lei, D. Lin, J. Liu et al., "Modified chloride diffusion model for concrete under the coupling effect of mechanical load and chloride salt environment," *AIP Advances*, vol. 8, no. 3, Article ID 035029, 2018.

[2] J. Ma, P. Yin, L. Huang, and Y. Liang, "The application of distinct lattice spring model to zonal disintegration within deep rock masses," *Tunnelling and Underground Space Technology*, vol. 90, pp. 144–161, 2019.

[3] C. Gong, W. Ding, K. Soga, and K. M. Mosalam, "Failure mechanism of joint waterproofing in precast segmental tunnel linings," *Tunnelling and Underground Space Technology*, vol. 84, pp. 334–352, 2019.

[4] W. Ding, C. Gong, K. M. Mosalam, and K. Soga, "Development and application of the integrated sealant test apparatus for sealing gaskets in tunnel segmental joints," *Tunnelling and Underground Space Technology*, vol. 63, pp. 54–68, 2017.

[5] M. Lei, D. Lin, C. Shi et al., "A structural calculation model of shield tunnel segment: heterogeneous equivalent beam model," *Advances in Civil Engineering*, vol. 2018, Article ID 9637838, , 2018.

[6] L. Huang, J. Ma, M. Lei, L. Liu, Y. Lin, and Z. Zhang, "Soil-water inrush induced shield tunnel lining damage and its stabilization: a case study," *Tunnelling and Underground Space Technology*, vol. 97, Article ID 103290, 2020.

[7] Z. Zhang and M. Zhang, "Mechanical effects of tunneling on adjacent pipelines based on galerkin solution and layered transfer matrix solution," *Soils and Foundations*, vol. 53, no. 4, pp. 557–568, 2013.

[8] F. H. Chehade and I. Shahrour, "Numerical analysis of the interaction between twin-tunnels: influence of the relative position and construction procedure," *Tunnelling and Underground Space Technology*, vol. 23, no. 2, pp. 210–214, 2008.

[9] T. Boonyarak and C. W. W. Ng, "Effects of construction sequence and cover depth on crossing-tunnel interaction," *Canadian Geotechnical Journal*, vol. 52, no. 7, pp. 851–867, 2015.

[10] C. Gong, W. Ding, K. M. Mosalam, S. Günay, and K. Soga, "Comparison of the structural behavior of reinforced concrete and steel fiber reinforced concrete tunnel segmental joints," *Tunnelling and Underground Space Technology*, vol. 68, pp. 38–57, 2017.

[11] S. Knothe, "Observations of surface movements under influence of mining and their theoretical interpretation," in *Proceedings of European Conference on Ground Movement*, pp. 210–218, 1957.

[12] M. Lei, D. Lin, Q. Huang, C. Shi, and L. Huang, "Research on the construction risk control technology of shield tunnel underneath an operational railway in sand pebble formation: a case study," *European Journal of Environmental and Civil Engineering*, vol. 24, no. 10, pp. 1558–1572, 2020.

[13] M. Lei, J. Liu, Y. Lin et al., "Deformation characteristics and influence factors of a shallow tunnel excavated in soft clay with high plasticity," *Advances in Civil Engineering*, vol. 2019, Article ID 7483628, , 2019.

[14] T. B. Celestino, R. A. M. P. Gomes, and A. A. Bortolucci, "Errors in ground distortions due to settlement trough adjustment," *Tunnelling and Underground Space Technology*, vol. 15, no. 1, pp. 97–100, 2000.

[15] Y.-S. Fang, C.-T. Wu, S.-F. Chen, and C. Liu, "An estimation of subsurface settlement due to shield tunneling," *Tunnelling and Underground Space Technology*, vol. 44, pp. 121–129, 2014.

[16] R. J. Mair, R. N. Taylor, and A. Bracegirdle, "Subsurface settlement profiles above tunnels in clays," *Geotechnique*, vol. 43, no. 2, pp. 361-362, 1993.

[17] R. B. Peck, "Deep excavations and tunnelling in soft ground," in *Proceedings of the 7th International Conference on Soil Mechanics and Foundation Engineering*, pp. 225–290, Mexico City, MX, USA, July 1969.

[18] C. Yoo and S.-B. Kim, "Three-dimensional numerical investigation of multifaced tunneling in water-bearing soft ground," *Canadian Geotechnical Journal*, vol. 45, no. 10, pp. 1467–1486, 2008.

[19] C. W. Ng, K. M. Lee, and D. K. Tang, "Three-dimensional numerical investigations of new austrian tunnelling method (NATM) twin tunnel interactions," *Canadian Geotechnical Journal*, vol. 41, no. 3, pp. 523–539, 2004.

[20] H. M. Shahin, T. Nakai, K. Ishii, T. Iwata, and S. Kuroi, "Investigation of influence of tunneling on existing building and tunnel: model tests and numerical simulations," *Acta Geotechnica*, vol. 11, no. 3, pp. 679–692, 2016.

[21] M. Hajjar, A. Nemati Hayati, M. M. Ahmadi et al., "Longitudinal settlement profile in shallow tunnels in drained conditions," *International Journal of Geomechanics*, vol. 15, no. 6, Article ID 04014097, 2015.

[22] N.-A. Do, D. Dias, and P. Oreste, "Three-dimensional numerical simulation of mechanized twin stacked tunnels in soft ground," *Journal of Zhejiang University Science A*, vol. 15, no. 11, pp. 896–913, 2014.

[23] C. Sagaseta, "Analysis of undraind soil deformation due to ground loss," *Géotechnique*, vol. 37, no. 3, pp. 301–320, 1987.

[24] K.-H. Park, "Analytical solution for tunnelling-induced ground movement in clays," *Tunnelling and Underground Space Technology*, vol. 20, no. 3, pp. 249–261, 2005.

[25] N. Loganathan and H. G. Poulos, "Analytical prediction for tunneling-induced ground movements in clays," *Journal of Geotechnical and Geoenvironmental Engineering*, vol. 124, no. 9, pp. 846–856, 1998.

[26] J. Fu, J. Yang, L. Yan, and S. M. Abbas, "An analytical solution for deforming twin-parallel tunnels in an elastic half plane," *International Journal for Numerical and Analytical Methods in Geomechanics*, vol. 39, no. 5, pp. 524–538, 2015.

[27] C. Shi, C. Cao, and M. Lei, "An analysis of the ground deformation caused by shield tunnel construction combining an elastic half-space model and stochastic medium theory," *KSCE Journal of Civil Engineering*, vol. 21, no. 5, pp. 1933–1944, 2017.

[28] K. H. Park, "Elastic solution for tunneling-induced ground movements in clays," *International Journal of Geomechanics*, vol. 4, no. 4, pp. 310–318, 2004.

[29] Z. Zhang, M. Zhang, Y. Jiang, Q. Bai, and Q. Zhao, "Analytical prediction for ground movements and liner internal forces induced by shallow tunnels considering non-uniform convergence pattern and ground-liner interaction mechanism," *Soils and Foundations*, vol. 57, no. 2, pp. 211–226, 2017.

[30] L. Tong, K. Xie, Y. Cheng et al., "Elastic solution of sallow tunnels in clays considering oval deformation of ground," *Rock and Soil Mechanics*, vol. 30, no. 2, pp. 393–398, 2009, in Chinese.

[31] C. Lin, T. Xia, R. Liang et al., "Estimation of shield tunnelling-induced ground surface settlements by virtual image technique," *Rock and Soil Mechanics*, vol. 36, no. 8, pp. 1438–1446, 2014, in Chinese.

[32] A. Verruijt, "A complex variable solution for a deforming circular tunnel in an elastic half-plane," *International Journal for Numerical and Analytical Methods in Geomechanics*, vol. 21, no. 2, pp. 77–89, 1997.

[33] A. Verruijt, "Deformations of an elastic half plane with a circular cavity," *International Journal of Solids and Structures*, vol. 35, no. 21, pp. 2795–2804, 1998.

[34] L.-Z. Wang, L.-L. Li, and X.-J. Lv, "Complex variable solutions for tunneling-induced ground movement," *International Journal of Geomechanics*, vol. 9, no. 2, pp. 63–72, 2009.

[35] J. S. Yang, B. C. Liu, and M. C. Wang, "Modeling of tunneling-induced ground surface movements using stochastic medium theory," *Tunnelling and Underground Space Technology*, vol. 19, no. 2, pp. 113–123, 2004.

[36] X. L. Yang and J. M. Wang, "Ground movement prediction for tunnels using simplified procedure," *Tunnelling and Underground Space Technology*, vol. 26, no. 3, pp. 462–471, 2011.

[37] A. Bobet, "Analytical solutions for shallow tunnels in saturated ground," *Journal of Engineering Mechanics*, vol. 127, no. 12, pp. 1258–1266, 2001.

[38] W.-I. Chou and A. Bobet, "Predictions of ground deformations in shallow tunnels in clay," *Tunnelling and Underground Space Technology*, vol. 17, no. 1, pp. 3–19, 2002.

[39] W. Yuan, H. Fu, J. Zhang et al., "Analytical prediction for tunneling-induced ground movements with modified deformation pattern," *International Journal of Geomechanics*, vol. 18, no. 6, Article ID 04018039, 2018.

[40] C. González and C. Sagaseta, "Patterns of soil deformations around tunnels: application to the extension of madrid metro," *Computers and Geotechnics*, vol. 28, no. 6-7, pp. 445–468, 2001.

[41] A. Verruijt and J. R. Booker, "Surface settlements due to ground loss and ovalisation of tunnel," *Géotechnique*, vol. 46, no. 4, pp. 753–756, 1996.

[42] R. K. Rowe and G. J. Kack, "A theoretical examination of the settlements induced by tunnelling: four case histories," *Canadian Geotechnical Journal*, vol. 20, no. 2, pp. 299–314, 1983.

[43] K. M. Lee, R. K. Rowe, and K. Y. Lo, "Subsidence owing to tunnelling. i. estimating the gap parameter," *Canadian Geotechnical Journal*, vol. 29, no. 6, pp. 929–940, 1992.

[44] H. S. Yu and R. K. Rowe, "Plasticity solutions for soil behaviour around contracting cavities and tunnels," *International Journal for Numerical and Analytical Methods in Geomechanics*, vol. 23, no. 12, pp. 1245–1279, 1999.

[45] Y. Hu, Q. Sun, and J. Han, "Linear elastic-perfectly plastic solution for cylindrical cavity contraction and its application," *Rock and Soil Mechanics*, vol. 33, no. 5, pp. 1438–1444, 2012, in Chinese.

[46] D. Sheng, S. Sloan, and H. Yu, "Practical implementation of critical state models in fem," *International Journal of Computer Mathematics*, vol. 80, no. 5, pp. 559–571, 1999.

[47] Z. Xu, *A Brief Tutorial on Elastic Mechanics*, Higher Education Press, Beijing, China, 2013, in Chinese.

[48] P. Timoshenko and J. N. Goodier, *Theory of Elasticity*, McGraw-Hill, New York, NY, USA, 1970.

[49] X. L. Jiang and Z. M. Zhao, "Application of image method in calculating tunneling-induced soil displacement," *Journal of Harbin Institute of Technology*, vol. 37, no. 6, pp. 801–803, 2005.

[50] J. H. L. Palmer and D. J. Belshaw, "Deformations and pore pressures in the vicinity of a precast, segmented, concrete-lined tunnel in clay," *Canadian Geotechnical Journal*, vol. 17, no. 2, pp. 174–184, 1980.

[51] A. P. Deane and R. H. Bassett, "The heathrow express trial tunnel," *Proceedings of the Institution of Civil Engineers-Geotechnical Engineering*, vol. 113, no. 3, pp. 144–156, 1995.

[52] N. Phienwej, "Ground movements in shield tunnelling in Bangkok soils," in *Proceedings of the 14th International on Soil Mechanics and Foundation Engineering*, pp. 1469–1472, Hamburg, Germany, September 1997.

[53] P. B. Attewell and I. W. Farmer, "Ground deformations resulting from shield tunnelling in london clay," *Canadian Geotechnical Journal*, vol. 11, no. 3, pp. 380–395, 1974.

[54] A. Ledesma and E. Romero, "Systematic back-analysis in tunnel excavation problems as a monitoring technique," *Proc. 14th Int. Conf. Soil Mech. Found. Eng*, vol. 3, pp. 1425–1428, 1997.

[55] C.-g. Lin, Z.-m. Zhang, S.-m. Wu, and F. Yu, "Key techniques and important issues for slurry shield under-passing embankments: a case study of Hangzhou Qiantang river tunnel," *Tunnelling and Underground Space Technology*, vol. 38, pp. 306–325, 2013.

[56] K. M. Lee, H. W. Ji, C. K. Shen, J. H. Liu, and T. H. Bai, "Ground response to the construction of shanghai metro tunnel-line 2," *Soils and Foundations*, vol. 39, no. 3, pp. 113–134, 1999.

[57] Y. Zhang, Z. Yin, and Y. Xu, "Analysis of surface deformation caused by shield tunnel," *Chinese Journal of Rock Mechanics and Engineering*, vol. 21, no. 3, pp. 388–392, 2002, in Chinese.

[58] X. Xie, Y. Yang, and M. Ji, "Analysis of ground surface settlement induced by the construction of a large-diameter shield-driven tunnel in shanghai, China," *Tunnelling and Underground Space Technology*, vol. 51, pp. 120–132, 2016.

[59] R. P. Chen, J. Zhu, W. Liu, and X. W. Tang, "Ground movement induced by parallel EPB tunnels in silty soils," *Tunnelling and Underground Space Technology*, vol. 26, no. 1, pp. 163–171, 2011.

[60] M. M. Maynar and L. M. Rodriguez, "Predicted versus measured soil movements induced by shield tunnelling in the madrid metro extension," *Canadian Geotechnical Journal*, vol. 42, no. 4, pp. 1160–1172, 2005.

[61] B. Zeng, D. Huang, and D. Gu, "3D Analysis of the elasticity calculation of ground deformation induced by shield tunnel construction," *Modern Tunnelling Technology*, vol. 6, pp. 63–69, 2015, in Chinese.

[62] P. S. Zhang and W. Yan, "Analysis of surface deformation by tunneling excavation under small strain," *Applied Mechanics and Materials*, vol. 94-96, pp. 1782–1786, 2011.

[63] R. J. Mair, "Tunnelling and geotechnics: new horizons," *Géotechnique*, vol. 58, no. 9, pp. 695–736, 2008.

[64] S.-M. Liao, J.-H. Liu, R.-L. Wang, and Z.-M. Li, "Shield tunneling and environment protection in shanghai soft ground," *Tunnelling and Underground Space Technology*, vol. 24, no. 4, pp. 454–465, 2009.

[65] X. Yi, R. K. Rowe, and K. M. Lee, "Observed and calculated pore pressures and deformations induced by an earth balance shield," *Canadian Geotechnical Journal*, vol. 30, no. 3, pp. 476–490, 1993.

[66] Y. Fang and C. Chen, "Subsidence in Taipei basin due to shield tunneling," in *Proceedings of the 10th Southeast Asian Geotechnical Engineering Conference*, pp. 501–506, Taipei, Taiwan, May 1990.

[67] X. Jiang, Y. Cui, Y. Li et al., "Measurement and simulation of ground settlements of Tianjin subway shield tunnel construction," *Rock and Soil Mechanics*, vol. 26, no. 10, pp. 1612–1616, 2005, in Chinese.

[68] G. W. Clough and B. Schmidt, "Design and performance of excavations and tunnels in soft clay," *Developments in Geotechnical Engineering*, vol. 20, pp. 567–634, 1981.

[69] M. P. O'Reilly and B. M. New, "Settlement above tunnels in the United Kingdom-their magnitude and prediction," in *Tunnelling 82, Proceedings of the 3rd International Symposium*, pp. 173–181, Brighton, London, UK, 1983.